Zoologischer Anzeiger 268 (2017) 11–18

Contents lists available at ScienceDirect

Zoologischer Anzeiger

journal homepage: www.elsevier.com/locate/jcz

Zoologischer Anzeiger

Research paper

Shape variation of prey-catching structures in geophilomorph centipedes: A preliminary investigation using geometric morphometrics

Matteo Baiocco[a], Lucio Bonato[a], Andrea Cardini[b,c], Giuseppe Fusco[a,*]

[a] Department of Biology, University of Padova, via U. Bassi 58/B, 35131 Padova, Italy
[b] Dipartimento di Scienze Chimiche e Geologiche, Università di Modena e Reggio Emilia, via Campi 103, 41125, Modena, Italy
[c] School of Anatomy, Physiology and Human Biology, The University of Western Australia, 35 Stirling Highway, Crawley WA 6009, Australia

ARTICLE INFO

Article history:
Received 6 October 2016
Received in revised form 27 April 2017
Accepted 28 April 2017
Available online 1 May 2017

Keywords:
Allometry
Chilopoda
Directional asymmetry
Feeding ecology
Morphological integration

ABSTRACT

Geophilomorph centipedes are common arthropod soil predators, but very little is known about their preying behaviour and their diet. Here we develop an exploratory morpho-functional approach to better understand their feeding habits, based on the morphology of feeding-related structures. Through geometric morphometrics, in a sample of five geophilomorph species, we investigated morphological variation in the three most conspicuous component structures of their prey-catching apparatus. At intra-specific level, we found no strong evidence for sexual dimorphism, left-right directional asymmetries and allometry across adult stages. At inter-specific level, shape differences in the feeding apparatus among the sample species were highly significant and large, even between two congeneric species. We also found a significant covariation between the shapes of the three structures, including those that do not directly articulate with each other, suggesting some degree of morphological integration between the different structures of the prey-catching apparatus. This study suggests the effectiveness and power of geometric morphometrics for the quantitative study of centipede functional morphology and provides a basis for wider comparative investigations on their phenotypic evolution.

1. Introduction

Geophilomorph centipedes are active soil predators feeding on other invertebrates, mainly in forest ecosystems through the world. At variance with other arthropod soil predators, like spiders and carabid beetles, which mainly catch prey above the surface and in the upper soil layers, geophilomorphs are mostly endogeic and are among the main top consumers in the food web of soil interstitial environment (Edgecombe and Giribet, 2007; Voigtländer, 2011).

However, despite their central role in most soil ecosystems, very little is known about their preying behaviour and their diet, because of their elusive habits and difficulties in laboratory rearing. Additionally, more than in other centipedes, feeding in geophilomorphs involves pre-digestion of the prey and intake of food by pharyngeal sucking (Koch and Edgecombe, 2012), so that the morphological analysis of the gut content is expected to be ineffective, as also confirmed by direct observation (F. Bortolin, personal communication).

Characteristic prey-catching appendages in centipedes are the venomous maxillipeds of the first trunk segment, the *forcipules*, which are also considered the most conspicuous morphological synapomorphy of the group (Borucki, 1996; Edgecombe and Giribet, 2007). In the geophilomorphs, the two paired forcipules are articulated to the anterior margin of a robust ventral sclerite, the *coxosternite*, to form what we will call here the *forcipular apparatus* (Fig. 1).

Geophilomorpha comprise more than a thousand species (Bonato et al., 2016) and, in comparison with all other centipede main clades (another two thousands species in total), they present higher diversity in size and shape of the forcipular apparatus, which might suggest a comparably greater disparity in their feeding habits (Maruzzo and Bonato, 2014).

The association between feeding habits and the morphology of feeding-related structures is a widespread form of adaptation, and morpho-functional investigations of mouthparts and other structures involved in food intake have been successfully applied to the

* Corresponding author.
E-mail addresses: mat.baiocco@gmail.com (M. Baiocco), lucio.bonato@unipd.it (L. Bonato), cardini@unimo.it (A. Cardini), giuseppe.fusco@unipd.it (G. Fusco).

http://dx.doi.org/10.1016/j.jcz.2017.04.010
0044-5231/

Fig. 1. Forcipular apparatus in five species of geophilomorph centipedes. Ventral view, after removal of the head. Scale bars 0.5 mm, 0.2 mm for *S. linearis*.

study of the feeding ecology in other groups of arthropods (e.g., Zetto Brandmayr et al., 1998 Sasakawa, 2016).

Descriptions and illustrations of the shape of the forcipular apparatus are available in the taxonomic literature for many geophilomorph species, as its component structures encompass important diagnostic characters. However, this information is mainly qualitative in nature and is based almost invariantly on a single or a few specimens per species. Actually, variation within species and differences between species have never been investigated with quantitative methods.

Here we investigate the three more conspicuous component structures of the forcipular apparatus of geophilomorphs through *geometric morphometrics*, a collection of analytical tools that provide a statistical description of biological forms in terms of their size and geometric shape (e.g., Cardini, 2013). Geometric morphometrics has been successfully employed for investigating shape variation in feeding-related structures in arthropods (e.g., Bai et al., 2015; Sasakawa, 2016), but it has been rarely applied to centipedes (Lopez Gutierrez et al., 2011; Siriwut et al., 2015) and never to geophilomorphs and to the entire forcipular apparatus. Thus, we carried out an exploratory investigation on the morphology of the forcipular apparatus in five geophilomorph species, representative of the main lineages of the group. We assessed the effect of several candidate sources of size and shape variation within species, and conducted some exploratory analyses on the variation between species. We also investigated the level of morphological integration among the component structures of the forcipular apparatus analysing the pattern of size and shape covariation among them.

2. Materials and methods

2.1. Sample

We examined 94 specimens belonging to five species of geophilomorph centipedes (Table 1; Fig. 1). The species were chosen to represent all the three major clades recognized in the Geophilomorpha (Placodesmata, Himantarioidea and Geophiloidea; Bonato et al., 2014a) and to include a pair of congeneric species. Specimens were identified with ChiloKey for the European species (Bonato et al., 2014b) and, for the only non-European species *T. nepalensis*, referring to the original description by Shinohara (1965). Specimens were collected from different localities within a narrow part of the entire range of the species, in order to minimize the effect of intraspecific geographical variation (Table 1). All specimens are conserved in 70% ethanol in the Bonato-Minelli collection (Department of Biology, University of Padova, Italy).

For each species we chose specimens with fully developed gonopods, in order to limit ontogenetic variation to the adult phase. Sex assignment was done on the basis of the shape of the gonopods.

2.2. Image acquisition

For obtaining clear photos of the forcipular apparatus, which is located beneath the head, the entire cephalic capsule was removed using entomological needles under a stereomicroscope. Specimens were then mounted on a microscope slide with ethylene glycol, the ventral side up. Each specimen was covered by a coverslip (smaller specimens) or by another microscope slide (larger specimens). The forcipular apparatus was photographed using a digital camera (LEICA DFC 400) mounted on a light microscope (LEICA DM LB). Images were acquired through the Leica Application Suite software (V.2.8.1) at a size of 2592 × 1944 pixels. As standard practice for controlling for measurement error (Viscosi and Cardini, 2011; and references therein), two images of each specimen were taken, each time following a new placement of the specimen on the slide. Sample positioning and image acquisition were carried out by the same person (MB) for all specimens.

2.3. Landmark choice and digitalization

The forcipular apparatus consists of several articulated component structures, whose relative position may vary and cannot be easily standardized, because of post-mortem body contraction and relative stiffening of the specimen in the storing liquid. Thus we analyzed its most conspicuous component structures separately. These are the *coxosternite* and, for each one of the two forcipules, the basal article or *trochanteroprefemur* and the apical article or *tarsungulum* (Bonato et al., 2010; Fig. 2). We digitized landmarks on both left and right sides of the coxosternite, as well as on both left and right forcipules. Landmarks on the same structure were chosen to be approximately coplanar, in order to mitigate against the error

Table 1
Sample composition.

Species	provenance	males	females	total
Tygarrup nepalensis Shinohara, 1965 [Placodesmata]	Nepal	8	9	17
Stigmatogaster gracilis (Meinert, 1870) [Himantarioidea]	NW Italy	12	8	20
Stenotaenia linearis (Koch,1835) [Geophiloidea]	N Italy	8	10	18
Strigamia acuminata (Leach, 1815) [Geophiloidea]	N and Central Italy	8	10	18
Strigamia crassipes (Koch, 1835) [Geophiloidea]	NW Italy	15	6	21

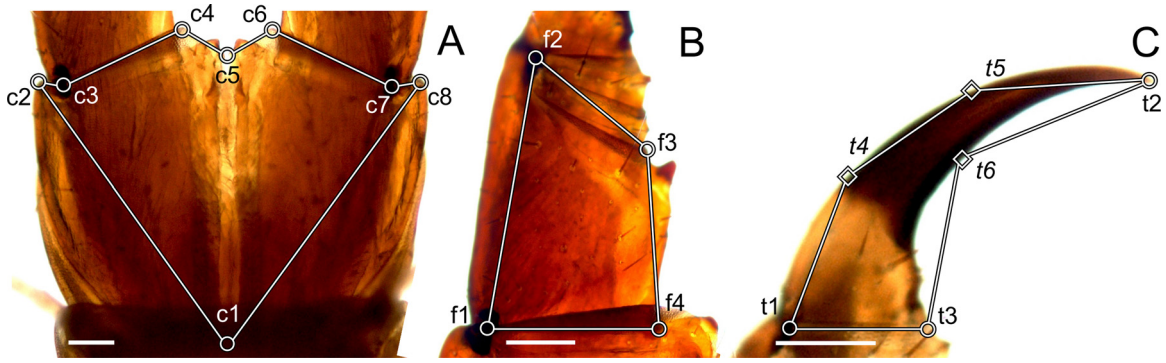

Fig. 2. Position of landmarks (circles) and semilandmarks (diamonds) on three structures of forcipular apparatus: (A) coxosternite; (B) right trochanteroprefemur; (C) right tarsungulum. Scale bars 0.2 mm.

Table 2
Landmarks and *semilandmarks* applied to three component structures of the forcipular apparatus.

structure	landmark/*semilandmark*	definition
coxosternite	c1	Medial point of the posterior edge of the coxosternite
	c2, c8	Antero-lateral corners of the coxosternite
	c3, c7	Tips of the coxosternal condyles (≡ f1)
	c4, c6	Antero-medial corners of the coxosternite
	c5	Medial notch of the anterior edge of the coxosternite
trochanteroprefemur	f1	Tip of the basal condyle of the trochanteroprefemur (≡ c3 or c7)
	f2	Ventral end of the hinge between the trochanteroprefemur and the tarsungulum (≡ t1)
	f3	Internal distal corner of the trochanteroprefemur
	f4	Internal basal corner of the trochanteroprefemur
tarsungulum	t1	Ventral end of the hinge between the trochanteroprefemur and the tarsungulum (≡ f2)
	t2	Tip of the tarsungulum
	t3	Internal basal corner of the tarsungulum
	t4	Point at one-third of the external edge of the tarsungulum (from the base)
	t5	Point at two-third of the external edge of the tarsungulum (from the base)
	t6	Mid-point of the internal edge of the tarsungulum

stemming from the projection of a three-dimensional structures onto the plane of the image (Cardini, 2014, and references therein). We used the following landmarks and semilandmarks (Table 2; Fig. 2): 8 landmarks for the coxosternite (c1–c8); 4 landmarks for each of the two trochanteroprefemora (f1–f4); 3 landmarks for each of the two tarsungula (t1–t3) and, to capture information on the internal and external curved edges of this sickle-like structure, 3 semilandmarks (t4–6). One landmark is shared between the coxosternite and each trochanteroprefemur (c3≡f1 right, c7≡f1 left) and one is shared between each trochanteroprefemur and its corresponding tarsungulum (f2≡t1).

TPS files were prepared using TPSUtil (ver. 1.58; Rohlf, 2015). Images were loaded in TPSDig 2 (ver. 2.17; Rohlf, 2015), where landmarks and semilandmarks were digitized on each image twice by the same person (MB) in different days. Thus, each individual was represented by 20 different raw datasets: five structures, each with two photos, which were digitized twice. This allowed to separately estimate the contribution of positioning and digitizing to measurement error (Klingenberg et al., 2002). The 2D approximation of the 3D structure was not included in the estimate of measurement error (Cardini, 2014) but, as we mentioned, this source of error was minimized by choosing approximately coplanar landmarks.

Semilandmarks represent a conceptually simple way of measuring regions without well-defined landmarks with a clear one to one anatomical correspondence (e.g., relatively smooth curves or surfaces, Gunz and Mitteroecker, 2013). They generally receive a specific mathematical treatment, which, in our case, was obtained by sliding them using the minimum squared Procrustes distance criterion in TPSRelw (ver. 1.54; Rohlf, 2015). This treatment increases the mathematical correspondence of these special points. However, as this procedure is not based on any biological model, semilandmarks lack the same type of clear mapping onto corresponding biological features, which is a property of traditional anatomical landmarks (Cardini and Loy, 2013). Results of semilandmark analyses should therefore be interpreted with caution. We limited the use of semilandmarks to the tarsungulum, a structure with only three homologous points, and kept their number at a minimum. Also, all the analyses on the tarsungulum were replicated on the configuration of the three landmarks only.

2.4. Geometric morphometrics and statistical analyses

Analyses were performed using geometric morphometric methods based on Procrustes superimposition, which standardizes size and minimizes positional differences to transform raw Cartesian coordinates into shape coordinates (Adams et al., 2013; Cardini, 2013). In each specimen, size was estimated as centroid size (CS), the square root of the sum of squared distances of the landmarks from their barycentre. When not stated otherwise, analyses were carried out using the package MorphoJ (ver. 1.06c, Klingenberg, 2011).

The coxosternite presents an internal plane of symmetry, and it is thus said to have *object symmetry*, i.e. a form of bilateral symmetry in which a structure is symmetric in itself. The trochanteroprefemora and the tarsungula are paired structures, and thus exhibit a different type of symmetry, generally referred to as *matching symmetry* (Klingenberg et al., 2002; Klingenberg, 2015). Procrustes methods allow to partition symmetric and asymmetric components of shape variation. Thus, directional and fluctuating asymmetry can be tested, as well as the differences among groups using symmetric shape.

Within-species sexual dimorphism and bilateral asymmetry were investigated using a Procrustes analysis of variance (Procrustes ANOVA) and a Multivariate analysis of variance (MANOVA),

Table 3
Intra-specific sexual dimorphism: ANOVA of the shape. Abbreviations: PT p, Pillai's Trace p-value; SS%, percentage of total sum of squares. Statistically significant p values ($p < 0.05$) are in bold.

	coxosternite			trochanteroprefemur				tarsungulum			
Species	SS%	F	p	SS%	F	p	PT p	SS%	F	p	PT p
T. nepalensis	1.0	0.25	0.956	6.2	1.53	0.205	0.313	4.8	1.08	0.381	0.850
S. gracilis	2.9	0.84	0.545	4.8	1.38	0.248	0.532	3.5	1.03	0.420	0.765
S. linearis	4.5	1.08	0.378	2.6	0.75	0.562	0.674	4.0	1.16	0.327	0.551
S. acuminata	9.2	2.27	**0.044**	8.2	2.80	**0.033**	0.523	1.3	0.42	0.906	0.269
S. crassipes	2.4	0.71	0.642	0.8	0.25	0.908	0.733	0.4	0.12	0.998	0.571

Table 4
Intra-specific directional asymmetries: MANOVA for coxosternite and ANOVA for trochanteroprefemur and tarsungulum. Abbreviations: PT p, Pillai's Trace p-value; SS%, percentage of total sum of squares. Statistically significant p values ($p < 0.05$) are in bold.

	coxosternite		trochanteroprefemur							tarsungulum						
	shape		size			shape				size			shape			
Species	SS%	PT p	SS%	F	p	SS%	F	p	PT p	SS%	F	p	SS%	F	p	PT p
T. nepalensis	1.33	0.062	0.01	0.17	0.684	0.52	0.51	0.729	0.150	0.24	2.78	0.115	1.48	1.17	0.321	0.271
S. gracilis	3.34	0.060	0.00	0.04	0.844	3.95	4.15	**0.004**	**0.008**	0.05	1.14	0.300	4.02	3.94	**<0.001**	**0.020**
S. linearis	0.72	0.110	0.01	0.57	0.459	1.67	2.10	0.090	0.315	<0.01	0.06	0.813	1.60	2.15	**0.035**	0.696
S. acuminata	0.67	0.384	0.07	3.75	0.070	3.80	3.62	**0.010**	0.131	0.17	4.06	0.060	2.58	1.83	0.076	0.196
S. crassipes	1.55	**0.028**	0.04	3.09	0.094	1.16	1.36	0.254	0.075	0.18	4.91	**0.038**	3.33	3.27	**0.002**	0.627

following the framework outlined by Klingenberg et al. (2002, and references therein). The main effect of sex was included in the within-species analysis together with the random effect of individual variation and those of directional and fluctuating asymmetry. The remaining variance in the model represented differences among replicas and therefore was used as our estimate of measurement error.

Within-species sexual dimorphism was further investigated after averaging replicas within individuals. Shape was regressed onto a sex dummy variable (females = −1 and males = 1). Significance of sexual dimorphism was estimated by the percentage of variance explained by the dummy variable and tested using 10000 permutations of the order of the individuals.

The same dataset obtained by averaging replicas within individuals, using samples with pooled sexes (as the effect on shape resulted negligible, see Results), was used to study allometry, inter-specific variation and size and shape covariation between the three structures.

Within-species allometry, i.e. the covariation between shape and size, was studied through a multivariate linear regression of shape variables onto centroid size (Mitteroecker et al., 2013), and tested using the same type of permutation test as in the regression of shape on sex. For geophilomorphs there are no reliable criteria to assign an individual to a given developmental stage (or instar, the period between two successive moults) when adult. Thus for each species we also computed the relative range of the size in our sample, as the ratio between the largest and the smallest centroid sizes, in order to weigh the contribution of ontogenetic allometry.

Inter-specific shape differences were explored with a canonical variate analysis (CVA) for shape, followed by pairwise permutation tests of mean differences, and with a between-groups principal component analysis (BG-PCA; Seetah et al., 2012, and references therein). A detailed introduction on morphometric applications of the discriminant analysis and canonical variate analysis is in Kovarovic et al. (2011).

Finally, size and shape covariation between the three structures (coxosternite, trochanteroprefemur and tarsungulum) was studied using Pearson's correlations for size and partial least squares (PLS) analysis for shape (Rohlf and Corti, 2000). In theory, the three structures could potentially have almost completely independent size and shape, one relative to the other, because even the two pairs that are in direct contact (coxosternite vs. trochanteroprefemur and trochanteroprefemur vs. tarsungulum; Fig. 2) have only one landmark in common. PLS analysis combines the shape coordinates to produce new variable axes that represent the largest amount of covariance between the couple of structures under evaluation. The significance of the RV coefficient (a multivariate equivalent of a correlation coefficient used in PLS analysis) was tested using a permutation test (with 10000 randomization rounds).

3. Results

3.1. Intra-specific variation

Within all species, Procrustes ANOVAs revealed a highly significant effect of the individual variation, which explains from 86% to 99% of the size total sum of squares, and from 47% to 66% of the shape total sum of squares. Measurement errors (specimen positioning plus digitalization errors) accounted for 0.07–1.2% of the size total sum of squares and 7–27% of shape total sum of squares, depending on the structure and the species (Supplementary material Tables S1–S8).

Sexual dimorphism. Procrustes ANOVAs of shape (Table 3, Supplementary material Tables S2, S4, S6, S8) revealed a marginally significant sexual dimorphism for *S. acuminata* only, with coxosternite and trochanteroprefemur on average slightly stouter in females than in males. The effect is considered marginally significant as it is no longer significant with a Bonferroni correction for multiple tests. Sex differences in size were not considered because the adult phase encompasses several developmental stages, and thus likely differences in sample composition between the two sexes can have a stronger impact on size than on the relatively more uniform shape.

Sexual dimorphism was also investigated through a permutation test on the symmetric component of the coxosternite, as well as on the trochanteroprefemur and tarsungulum. Mean shape differences between sexes resulted non-significant for the three structures in all species (for all 15 tests, $p > 0.05$, 10000 randomization rounds).

Bilateral asymmetry. The MANOVA performed on the coxosternite (asymmetric component, Table 4, Supplementary material Table S9) revealed a significant directional asymmetry only for *S. crassipes*, where however it explained less than 2% of the total shape variance. The ANOVAs performed on the trochanteroprefemur and the tarsungulum (Table 4) revealed significant directional asymmetry in *S. gracilis*, *S. acuminata* and *S. crassipes*, which never accounted

for more than 4% of total shape variation. In the tarsungulum of *S. crassipes*, the only case of significant size variation revealed by the ANOVA, the right tarsungulum is on average 2.7% larger than the left one. In no species significant directional asymmetry was found consistently across the three structures, and only the left-right shape differences in the tarsungulum of *S. gracilis* and *S. crassipes* resulted significant after Bonferroni Correction for multiple tests.

The shape Procrustes ANOVA also showed highly significant bilateral fluctuating asymmetry in all species and structures ($p < 0.0001$, significant even if Bonferroni corrected; Supplementary material Tables S2–S8), where it accounted for 0.2–1.4% of total size variation and 7.5–23.9% of total shape variation.

Allometry. Only the symmetric component of the shape of the coxosternite of *S. gracilis* and *S. crassipes* showed a significant change in shape with size (Table 5), but none of those regressions was significant after a Bonferroni correction for multiple tests. Instead, *S. linearis* and *S. acuminata* presented significant allometry at the level of the tarsungulum, with *S. acuminata* still significant after a Bonferroni correction.

Significant results seem however to depend on a few influential points with high leverage. Excluding from the regression analysis a few small specimens, thus reducing the relative range of the centroid size to a value slightly below 2.0, whilst still putatively including 4–6 adult to adult moults (see Discussion), all allometric relationships become non-significant.

3.2. Inter-specific variation

The canonical variate analysis revealed shape differences between all species (Table 6), which were highly significant in all pairwise tests ($p < 0.0001$, explaining 34–95% of total shape variance) and remained significant also after the Bonferroni correction for multiple tests. This pattern was confirmed by BG-PCA as well (results not shown). Likewise, a replica of CVA for the tarsungulum excluding the three semilandmarks gave significant pairwise shape distances among the five species, although, on average, smaller than those including the semilandmaks (results not shown).

For the coxosternite, the first canonical variate explains 70% of the between-species shape variance (Fig. 3A). This axis of variation goes from a coxosternite with more rearward condyle position, the anterior edge medially more projecting and with an inconspicuous notch (see *S. gracilis* and *T. nepalensis*) to a coxosternite with more forward condyle position, a less projecting anterior edge and the medial notch rather sunken (see *S. acuminata*). The second canonical variate (which explains 18% of variance) describes shape variation in the coxosternite from relatively stout (see *S. gracilis* and *S. acuminata*) to rather elongated (see *S. linearis*).

For the trochanteroprefemur, the first canonical variate explains 80% of the between-species shape variance (Fig. 3B). This axis of variation ranges from a slender (see *T. nepalensis*) to a stouter (see *S. gracilis* and *S. linearis*) trochanteroprefemur. The second canonical variate (which explains 16% of variance) describes shape variation that mainly consists in the relative shortening of the external edge of the trochanteroprefemur with respect to its internal edge (see *S. crassipes* vs. *S. linearis*).

For the tarsungulum, the first canonical variate explains 45% of the between-species shape variance (Fig. 3C). The main effect of shape change along this direction is an increase in the curvature of the tarsungulum (see *S. gracilis* vs. *S. crassipes*). The second canonical variate (which accounts for 32% of the overall shape variance) describes a reduction in the thickness of tarsungulum, accompanied by a relative extension of its internal edge (see *T. nepalensis* vs. *S. linearis*).

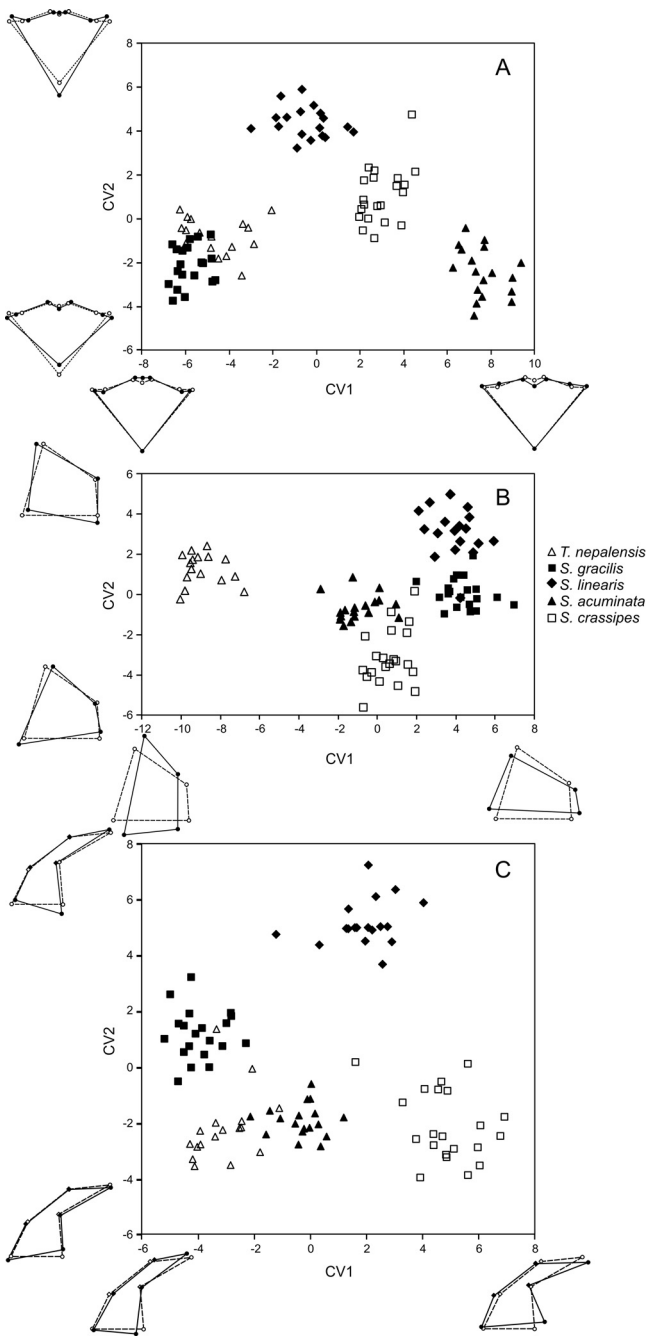

Fig. 3. Differences between the five species in relation to the first two variates from canonical variate analysis on the three structures of the forcipular apparatus: (A) coxosternite; (B) trochanteroprefemur; (C) tarsungulum. Shape variation along the two axes is shown as solid line wire frames with respect to the average shape (dashed line wire frames).

3.3. Size and shape covariation between structures

The analysis of size correlation and shape covariation between different structures produced concordant results (Table 7). Both the three correlation coefficients (size) and the three RV coefficients (shape) resulted highly significant ($p < 0.0001$). The first two PLS axes accounted for 94–99% of the squared covariance.

Considering the first shape PLS axis (accounting for 78–95% of squared covariance), a relatively elongated coxosternite corresponds to an elongated trochanteroprefemur, which corresponds to a more oblique tarsungulum with respect to its base. A coxoster-

Table 5
Intra-specific allometry: multivariate regression of shape on centroid size. Abbreviations: SR, size relative range, computed as the ratio between the largest and the smallest centroid size in the species sample; var%, percentage of explained shape variance. Statistically significant p values ($p < 0.05$) are in bold.

	coxosternite					trochanteroprefemur			tarsungulum		
Species	Symmetric		Asymmetric								
	var%	p	var%	p	SR	var%	p	SR	var%	p	SR
T. nepalensis	3.63	0.650	1.27	0.865	2.36	3.78	0.661	2.44	12.62	0.090	2.31
S. gracilis	16.04	**0.027**	9.52	0.117	2.02	9.97	0.399	1.88	10.12	0.123	1.94
S. linearis	2.68	0.728	7.82	0.248	2.47	5.78	0.132	2.35	21.22	**0.018**	2.41
S. acuminata	4.81	0.471	5.41	0.435	2.15	3.52	0.565	2.09	21.81	**0.002**	2.19
S. crassipes	19.03	**0.012**	0.89	0.942	3.60	3.89	0.488	3.58	4.48	0.429	3.51

Table 6
Pairwise Procrustes distances among the five species.

	coxosternite				trochanteroprefemur				tarsungulum			
	T. nep.	*S. gra.*	*S. lin.*	*S. acu.*	*T. nep.*	*S. gra.*	*S. lin.*	*S. acu.*	*T. nep.*	*S. gra.*	*S. lin.*	*S. acu.*
S. gracilis	0.1643				0.3786				0.1079			
S. linearis	0.0839	0.1904			0.3946	0.0943			0.1144	0.1028		
S. acuminata	0.1538	0.1407	0.1434		0.2325	0.1508	0.1917		0.0588	0.1301	0.0914	
S. crassipes	0.1181	0.1291	0.1006	0.0854	0.2987	0.1315	0.1901	0.0836	0.1786	0.2079	0.1446	0.1252

Table 7
Pairwise correlation coefficients for size and RV coefficients for shape among the three structures.

	size		shape	
	coxosternite	trochanteroprefemur	coxosternite	trochanteroprefemur
trochanteroprefemur	0.909		0.208	
tarsungulum	0.954	0.873	0.258	0.273

nite with the anterior edge medially more projecting corresponds to a less arched tarsungulum.

4. Discussion

The aim of this study was an exploratory investigation on the morphological variation of the forcipular apparatus in a sample of geophilomorph species. More specifically, we examined several candidate sources of shape variation both within and between species.

4.1. Intra-specific variation

Sexual dimorphism. To the best of our knowledge, there are no reports of any evidence of sexual dimorphism at the level of the feeding apparatus in geophilomorph centipedes, and our analyses fundamentally concur with these previous qualitative observations. A possible exception is provided by the shape of the coxosternite in *S. acuminata* (Table 3). However, the difference between the two sexes, although significant, is nonetheless quite modest. Moreover, this result is not confirmed by the permutation test and is non-significant if Bonferroni corrected. Thus, we can tentatively conclude that in the investigated species the feeding apparatus does not show appreciable shape differences between sexes.

Asymmetry. Directional asymmetries, i.e. consistent differences in size and/or shape between the two sides of a structure with bilateral symmetry, or between two paired structures, are not uncommon in Metazoa (Palmer, 1996) and are known for most major phyla, including Arthropoda, and several developmental biology model organisms. However, in the Chilopoda, directional left-right asymmetries have been reported only for the number of teeth in the mandible of the Scopendromorpha (Attems, 1930).

We found scattered evidence of directional asymmetry in the examined species. Size asymmetry was marginally significant only for the tarsungulum in *S. crassipes*, while shape asymmetry was apparent in one or two structures for all species to the exclusion of *T. nepalensis*. In all cases, the variation explained by left-right differences was relatively modest and in no species significant directional asymmetry involves coherently the three structures. Thus, overall, there seems to be no strong evidence of directional asymmetries in the forcipular apparatus of the investigated species. Actually, the position of the two sickled extremities of the forcipules can only be partially controlled during image acquisition. Due to the relative stiffness of the specimens, it is possible that some modest differential inclination of these structures with respect to the optical plane of the microscope is systematically introduced. This bias can result particularly problematic for the appearance of the curvature of the tarsungulum, which is a relevant component of its shape. In effect, the levels of explained variance in the Procrustes ANOVA of the shape of the tarsungulum without the semilandmarks tends to be smaller (Supplementary material Tables S6, S8). We checked for a possible effect of the slight overlap of the tips of the forcipules that is observed in some individuals (in ventral view, either the right one overlying the left one, or vice versa, as for instance in *S. linearis* in Fig. 1), but we found none.

The Procrustes ANOVA revealed also the presence of fluctuating asymmetries, i.e. random deviations from bilateral symmetry (Klingenberg 2015), both in size and in shape. However, although significant, size and composition of our samples are not adequate for hypothesis testing about its origin or covariation with other variables, thus we refrained from any further quantitative analysis on this asymmetry component.

The presence of left-right asymmetry in the forcipules definitely needs further investigation in much larger samples and probably adopting more invasive procedure of dissection, to allow better positioning control during image acquisition.

Allometry. Within-species, size-related shape variation can have two main sources: variation across individuals at different developmental stages (ontogenetic allometry) and variation across individuals at the same developmental stage (static allometry) (Cock, 1966). In geophilomorphs it is not possible to assign an

adult individual to a given developmental stage. Any sample of adult specimens will thus potentially present a mix of static and ontogenetic allometry that cannot be clearly separated.

We found scattered evidence of allometry of modest magnitude in our samples, occurring in no more than one structure for a single species, which also differed depending on the species. Additionally, in consideration of the fact that size variation is substantial in all species samples, possibly corresponding to several adult-to-adult moults (4–8, on the basis of an approximate per-moult growth rate of 1.15; Minelli and Fusco, 2013), and that a reduction of the size range in the samples turn allometric relationships into non-significant ones, there seems to be reasons to suspect that the observed size-related shape variation might mainly stem from variation across stages.

Overall, there is no strong evidence of allometry for the forcipular apparatus across adult stages in the species of our sample. On this subject too, future studies on more species and larger samples, including the largest possible representation of adult stages, might help to clarify whether this is a common feature of the Geophilomorpha.

4.2. Inter-specific variation

Shape differences in the feeding apparatus among the five species are large, as suggested by the canonical variate analysis (Fig. 3) and all other tests and analyses. This matches our expectations, as, for an exploratory study of the potential of geometric morphometrics applied to the feeding apparatus of the geophilomorphs, the species sample had been intentionally selected to represent a wide spectrum of shapes within the group. However, the landmark-based analyses resulted effective also in detecting shape differences between the two congeneric species, *Strigamia acuminata* and *S. crassipes*. Notably, greater similarity between congeneric species is observed in the coxosternite and in the trochanteroprefemur, but not at the level of the distalmost article of the forcipules, the tarsungulum.

Taken as a whole, shape differences between the two closely related congeneric species are of a magnitude comparable to those recorded among the other species of the sample, which are phylogenetically more distant from one another. This might indicate the overall shape of the forcipular apparatus to be relatively labile in evolution, likely disposed to adapt to different environmental conditions. However, only a larger comparative study, based on the phylogeny of the group, will possibly validate this conjecture.

4.3. Size and shape covariation between structures

We found a significant size and shape covariation between the three structures. Remarkably the covariation regards also the shape of coxosternite vs. tarsungulum, two structures that do not directly articulate with each other. This suggests some degree of morphological integration between the structures of the forcipular apparatus that does not depend on the pure mechanical constrains imposed by arthropod articulated joints.

4.4. Final remarks

In this preliminary study on the morphological variation of the prey-catching apparatus of geophilomorph centipedes, overall the quantification of size and shape variation showed no appreciable effects of either sex, body side and allometry at intra-specific level. This is nonetheless accompanied by sizable morphological differences among the species, even within the same genus.

Although the analysis of inter-specific variation is based on a small sample of species, the combination of the results at intra- and inter-specific levels showed that the methodological protocol, which includes the selection of the structures to be examined, the use of 2D geometric morphometrics and the specific choice of landmarks and semilandmarks, can evidently detect morphological differences at different taxonomic levels. This could be profitably applied in wider inter-specific studies, and possibly in a broader taxonomic context, significantly contributing to the study of centipede functional morphology and its evolution.

Acknowledgments

We thank F. Bortolin for sharing her unpublished data on geophilomorph gut content. This work was supported by the Italian Ministry of Education, University and Research (MIUR) [grant number 60A06-0281/10].

Appendix A. Supplementary data

Supplementary data associated with this article can be found, in the online version, at http://dx.doi.org/10.1016/j.jcz.2017.04.010.

References

Adams, D.C., Rohlf, F.J., Slice, D.E., 2013. A field comes of age: geometric morphometrics in the 21st century. Hystrix 24, 7–14.
Attems, C., 1930. Myriapoda 2. Scolopendromorpha. In: Schulze, F.E., Kükenthal, W. (Eds.), Das Tierreich, 54. Walter de Gruyter, Berlin, pp. 1–308.
Bai, M., Li, S., Lu, Y., Yang, H., Tong, Y., Yang, X., 2015. Mandible evolution in the Scarabaeinae (Coleoptera: Scarabaeidae) and adaptations to coprophagous habits. Front. Zool. 12, 30.
Bonato, L., Chagas Junior, A., Edgecombe, G.D., Lewis, J.G.E., Minelli, A., Pereira, L.A., Shelley, R.M., Stoev, P., Zapparoli, M., 2016. ChiloBase 2.0 – A World Catalogue of Centipedes (Chilopoda) (Available at http://chilobase.biologia.unipd.it).
Bonato, L., Drago, L., Murienne, J., 2014a. Phylogeny of Geophilomorpha (Chilopoda) inferred from new morphological and molecular evidence. Cladistics 30, 485–507.
Bonato, L., Edgecombe, G.D., Lewis, J.G.E., Minelli, A., Pereira, L.A., Shelley, R.M., Zapparoli, M., 2010. A common terminology for the external anatomy of centipedes (Chilopoda). Zookeys 69, 17–51.
Bonato, L., Minelli, A., Lopresti, M., Cerretti, P., 2014b. ChiloKey, an interactive identification tool for the geophilomorph centipedes of Europe. Zookeys 443, 1–9.
Borucki, H., 1996. Evolution und phylogenetisches System der Chilopoda (Mandibulata, Tracheata). Verh. Naturwiss. Ver. Hambg. 35, 95–226.
Cardini, A., 2013. Geometric morphometrics. In: UNESCO-EOLSSJointCommittee (Ed.), Encyclopedia of Life Support Systems. Biological science fundamental and systematics, Oxford, UK (Available at: http://www.eolss.net/TOC/C03-BrowseContents.aspx).
Cardini, A., 2014. Missing the third dimension in geometric morphometrics: how to assess if 2D images really are a good proxy for 3D structures? Hystrix 25, 63–72.
Cardini, A., Loy, A., 2013. On growth and form in the computer era: from geometric to biological morphometrics. Hystrix 24, 1–5.
Cock, A.G., 1966. Genetical aspects of metrical growth and form in animals. Quart. Rev. Biol. 41, 131–190.
Edgecombe, G.D., Giribet, G., 2007. Evolutionary biology of centipedes (Myriapoda: Chilopoda). Ann. Rev. Ent. 52, 151–170.
Gunz, P., Mitteroecker, P., 2013. Semilandmarks: a method for quantifying curves and surfaces. Hystrix 24, 103–109.
Klingenberg, C.P., 2011. MorphoJ: an integrated software package for geometric morphometrics. Mol. Ecol. 11, 353–357.
Klingenberg, C.P., 2015. Analyzing fluctuating asymmetry with geometric morphometrics: concepts, methods, and applications. Symmetry 7, 843–934.
Klingenberg, C.P., Barluenga, M., Meyer, A., 2002. Shape analysis of symmetric structures: quantifying variation among individuals and asymmetry. Evolution 56, 1909–1920.
Koch, M., Edgecombe, G.D., 2012. The preoral chamber in geophilomorph centipedes: comparative morphology, phylogeny, and the evolution of centipede feeding structures. Zool. J. Linn. Soc. 165, 1–62.
Kovarovic, K., Aiello, L.C., Cardini, A., Lockwood, C.A., 2011. Discriminant function analyses in archaeology: are classification rates too good to be true? J. Arch. Sci. 38, 3006–3018.
Lopez Gutierrez, B., MacLeod, N., Edgecombe, G.D., 2011. Detecting taxonomic signal in an under-utilised character system: geometric morphometrics of the forcipular coxae of Scutigeromorpha (Chilopoda). In: Mesibov, R., Short, M. (Eds.), Proceedings of the 15th International Congress of Myriapodology, 18–22 July 2011, Brisbane, Australia. ZooKeys 156: 49–66.
Maruzzo, D., Bonato, L., 2014. Morphology and diversity of the forcipules in *Strigamia* centipedes (Chilopoda, Geophilomorpha). Arthr. Str. Dev. 43, 17–25.

Minelli, A., Fusco, G., 2013. Arthropod post-embryonic development. In: Minelli, A., Boxshall, G., Fusco, G. (Eds.), Arthropod Biology and Evolution. Molecules, Development, Morphology. Springer Verlag, Berlin Heidelberg, pp. 91–122.
Mitteroecker, P., Gunz, P., Windhager, S., Schaefer, K., 2013. A brief review of shape, form, and allometry in geometric morphometrics, with applications to human facial morphology. Hystrix 24, 59–66.
Palmer, A.R., 1996. From symmetry to asymmetry: phylogenetic patterns of asymmetry variation in animals and their evolutionary significance. Proc. Natl. Acad. Sci. USA 93, 14279–14286.
Rohlf, F.J., 2015. The tps series of software. Hystrix 26, 9–12.
Rohlf, F.J., Corti, M., 2000. Use of two-block partial least-squares to study covariation in shape. Syst. Biol. 49, 740–753.
Sasakawa, K., 2016. Utility of geometric morphometrics for inferring feeding habit from mouthpart morphology in insects: tests with larval Carabidae (Insecta: Coleoptera). Biol. J. Linn. Soc. 118, 394–409.
Seetah, T.K., Cardini, A., Miracle, P.T., 2012. Can *morphospace* shed light on cave bear spatial-temporal variation? Population dynamics of *Ursus spelaeus* from Romualdova pećina and Vindija, (Croatia). J. Arch. Sci. 39, 500–510.
Shinohara, K., 1965. A new species of Chilopoda from Himalaya. J. Coll. Arts Sci. Chiba Univ. (Nat. Sci.) 4, 303–306.
Siriwut, W., Edgecombe, G.D., Sutcharit, C., Panha, S., 2015. The centipede genus *Scolopendra* in mainland Southeast Asia: molecular phylogenetics, geometric morphometrics and external morphology as tools for species delimitation. PLoS One 10, e0135355.
Viscosi, V., Cardini, A., 2011. Leaf morphology, taxonomy and geometric morphometrics: a simplified protocol for beginners. PLoS One 6, e25630.
Voigtländer, K., 2011. Chilopoda – Ecology. In: Minelli, A. (Ed.), Treatise on Zoology – Anatomy, Taxonomy, Biology. The Myriapoda, Volume 1. Brill Leiden, pp. 309–325.
Zetto Brandmayr, T., Giglio, A., Marano, I., Brandmayr, P., 1998. Morphofunctional and ecological features in carabid (Coleoptera) larvae. In: Ball, G.E., Casale, A., Vigna Taglianti, A. (Eds.), Phylogeny and classification of Caraboidea. XX I.C.E. Atti Museo Regionale di Scienze Naturali, Torino, pp. 449–499.

Shape variation of prey-catching structures in geophilomorph centipedes: a preliminary investigation using geometric morphometrics

Matteo Baiocco, Lucio Bonato, Andrea Cardini, Giuseppe Fusco

Supplementary tables

Supplementary Table 1. Procrustes ANOVA of the size of the forcipular coxosternite.

Species	Effect	SS	MS	df	F	p
T. nepalensis	Sex	57639.98	57639.98	1	0.09	0.7698
	Individual	9732885.70	648859.05	15	2689.65	<0.0001
	Residual	12303.37	241.24	51		
S. gracilis	Sex	165536.55	165536.55	1	2.13	0.1616
	Individual	1398268.86	77681.60	18	3551.81	<0.0001
	Residual	1312.26	21.87	60		
S. linearis	Sex	536766.23	536766.23	1	0.71	0.4112
	Individual	12062151.37	753884.46	16	1557.05	<0.0001
	Residual	26145.40	484.17	54		
S. acuminata	Sex	31057.90	31057.90	1	0.59	0.4531
	Individual	840321.93	52520.12	16	270.80	<0.0001
	Residual	10472.93	193.94	54		
S. crassipes	Sex	303067.35	303067.35	1	0.55	0.4683
	Individual	10513580.17	553346.32	19	878.15	<0.0001
	Residual	39698.13	630.13	63		

Supplementary Table 2. Procrustes ANOVA of the shape of the forcipular coxosternite.

Species	Effect	SS	MS	df	F	p
T. nepalensis	Sex	0.0011	0.00019	6	0.25	0.9562
	Individual	0.0659	0.00073	90	3.19	<0.0001
	Side	0.0014	0.00024	6	1.03	0.4094
	Ind * Side	0.0220	0.00023	96	8.50	<0.0001
	Residual	0.0165	2.7E-05	612		
S. gracilis	Sex	0.0065	0.0011	6	0.84	0.5447
	Individual	0.1394	0.0013	108	3.75	<0.0001
	Side	0.0074	0.0012	6	3.59	0.0027
	Ind * Side	0.0392	0.0003	114	8.54	<0.0001
	Residual	0.0290	4.0E-05	720		
S. linearis	Sex	0.0079	0.0013	6	1.08	0.3782
	Individual	0.1164	0.0012	96	9.43	<0.0001
	Side	0.0013	0.0002	6	1.64	0.1450
	Ind * Side	0.0130	0.0001	102	2.24	<0.0001
	Residual	0.0372	5.7E-05	648		
S. acuminata	Sex	0.0383	0.0064	6	2.27	0.0435
	Individual	0.2705	0.0028	96	9.23	<0.0001
	Side	0.0028	0.0005	6	1.53	0.1749
	Ind * Side	0.0311	0.0003	102	2.7	<0.0001
	Residual	0.0733	0.0001	648		
S. crassipes	Sex	0.0093	0.0015	6	0.71	0.6424
	Individual	0.2486	0.0022	114	6.59	<0.0001
	Side	0.0059	0.0010	6	2.99	0.0094
	Ind * Side	0.0397	0.0003	120	3.16	<0.0001
	Residual	0.0791	0.0001	756		

Supplementary Table 3. Procrustes ANOVA of the size of the forcipular trochanteroprefemur.

Species	Effect	SS	MS	df	F	p
T. nepalensis	Sex	4647.95	4647.95	1	0.01	0.9047
	Individual	4706890.05	313792.67	15	212.86	<0.0001
	Side	253.52	253.52	1	0.17	0.6839
	Ind *Side	23586.27	1474.14	16	27.83	<0.0001
	Residual	5403.04	52.97	102		
S. gracilis	Sex	54596.12	54596.12	1	2.25	0.1512
	Individual	437248.54	24291.59	18	75.34	<0.0001
	Side	12.85	12.85	1	0.04	0.8439
	Ind *Side	6125.83	322.41	19	34.22	<0.0001
	Residual	1130.73	9.42	120		
S. linearis	Sex	96762.12	96762.12	1	0.56	0.4657
	Individual	2772103.47	173256.47	16	461.14	<0.0001
	Side	215.87	215.87	1	0.57	0.4588
	Ind *Side	6387.12	375.71	17	4.38	<0.0001
	Residual	9258.52	85.73	108		
S. acuminata	Sex	7827.94	7827.94	1	0.41	0.5302
	Individual	304303.03	19018.94	16	321.93	<0.0001
	Side	221.31	221.31	1	3.75	0.0697
	Ind *Side	1004.33	59.08	17	6.31	<0.0001
	Residual	1011.66	9.37	108		
S. crassipes	Sex	72093.46	72093.46	1	0.37	0.5487
	Individual	3673359.64	193334.72	19	402.76	<0.0001
	Side	1482.00	1482.00	1	3.09	0.0942
	Ind *Side	9600.40	480.02	20	10.82	<0.0001
	Residual	5592.30	44.38	126		

Supplementary Table 4. Procrustes ANOVA of the shape of the forcipular trochanteroprefemur.

Species	Effect	SS	MS	df	F	p	Pillai's Trace	Pillai's Trace p
T. nepalensis	Sex	0.0212	0.0053	4	1.53	0.2049	0.31	0.3127
	Individual	0.2081	0.0035	60	3.95	<0.0001	3.14	<0.0001
	Side	0.0018	0.0004	4	0.51	0.7291	0.38	0.1498
	Ind * Side	0.0562	0.0009	64	6.54	<0.0001	1.78	<0.0001
	Residual	0.0547	0.0001	408				
S. gracilis	Sex	0.0249	0.0062	4	1.38	0.2479	0.18	0.5323
	Individual	0.3244	0.0045	72	3.60	<0.0001	2.96	<0.0001
	Side	0.0208	0.0052	4	4.15	0.0043	0.56	0.0080
	Ind * Side	0.0950	0.0013	76	9.98	<0.0001	2.37	<0.0001
	Residual	0.0601	0.0001	480				
S. linearis	Sex	0.0160	0.0040	4	0.75	0.5615	0.15	0.6743
	Individual	0.3413	0.0053	64	4.33	<0.0001	3.01	<0.0001
	Side	0.0103	0.0026	4	2.10	0.0904	0.27	0.3147
	Ind * Side	0.0837	0.0012	68	3.17	<0.0001	1.33	<0.0001
	Residual	0.1678	0.0004	432				
S. acuminata	Sex	0.0398	0.0010	4	2.80	0.0332	0.21	0.5226
	Individual	0.2277	0.0036	64	2.79	<0.0001	2.71	0.0006
	Side	0.0185	0.0046	4	3.62	0.0098	0.38	0.1305
	Ind * Side	0.0867	0.0013	68	4.89	<0.0001	1.50	<0.0001
	Residual	0.1125	0.0003	432				
S. crassipes	Sex	0.0050	0.0013	4	0.25	0.9078	0.11	0.7332
	Individual	0.3770	0.0050	76	3.82	<0.0001	2.87	<0.0001
	Side	0.0071	0.0018	4	1.36	0.2540	0.38	0.0752
	Ind * Side	0.1040	0.0013	80	5.52	<0.0001	1.86	<0.0001
	Residual	0.1187	0.0003	504				

Supplementary Table 5. Procrustes ANOVA of the size of the forcipular tarsungulum, with semilandmarks.

Species	Effect	SS	MS	df	F	p
T. nepalensis	Sex	406.36	406.36	1	0.00	0.9672
	Individual	3487170.89	232478.06	15	75.46	<0.0001
	Side	8554.25	8554.25	1	2.78	0.1151
	Ind *Side	49289.74	3080.61	16	18.68	<0.0001
	Residual	16818.84	164.89	102		
S. gracilis	Sex	90379.69	90379.69	1	2.69	0.1186
	Individual	605711.82	33650.66	18	103.34	<0.0001
	Side	370.25	370.25	1	1.14	0.2996
	Ind *Side	6186.98	325.63	19	36.76	<0.0001
	Residual	1062.95	8.86	120		
S. linearis	Sex	198195.30	198195.30	1	0.64	0.4341
	Individual	4926786.09	307924.13	16	540.51	<0.0001
	Side	33.05	33.05	1	0.06	0.8126
	Ind *Side	9684.85	569.70	17	18.26	<0.0001
	Residual	3368.99	31.19	108		
S. acuminata	Sex	5709.41	5709.41	1	0.2	0.6613
	Individual	458516.26	28657.27	16	153.49	<0.0001
	Side	758.73	758.73	1	4.06	0.0599
	Ind *Side	3173.91	186.70	17	6.18	<0.0001
	Residual	3260.90	30.19	108		
S. crassipes	Sex	61830.59	61830.59	1	0.38	0.5473
	Individual	3129024.99	164685.53	19	136.99	<0.0001
	Side	5907.46	5907.46	1	4.91	0.0384
	Ind *Side	24043.83	1202.19	20	37.45	<0.0001
	Residual	4044.76	32.10	126		

Supplementary Table 6. Procrustes ANOVA of the shape of the forcipular tarsungulum, with semilandmarks.

Species	Effect	SS	MS	df	F	p	Pillai's Trace	Pillai's Trace p
T. nepalensis	Sex	0.0187	0.0023	8	1.08	0.3807	0.32	0.8503
	Individual	0.2591	0.0021	120	3.49	<0.0001	4.73	0.0080
	Side	0.0058	0.0007	8	1.17	0.3206	0.58	0.2706
	Ind * Side	0.0792	0.0006	128	16.96	<0.0001	4.73	<0.0001
	Residual	0.0298	0.00004	816				
S. gracilis	Sex	0.0077	0.0010	8	1.03	0.4196	0.30	0.7654
	Individual	0.1351	0.0009	144	3.30	<0.0001	4.68	0.0082
	Side	0.0090	0.0011	8	3.94	0.0003	0.71	0.0199
	Ind * Side	0.0432	0.0003	152	9.74	<0.0001	3.87	<0.0001
	Residual	0.0280	0.00003	960				
S. linearis	Sex	0.0060	0.0008	8	1.16	0.3269	0.45	0.5514
	Individual	0.0830	0.0006	128	4.60	<0.0001	5.18	<0.0001
	Side	0.0024	0.0003	8	2.15	0.0353	0.35	0.6959
	Ind * Side	0.0192	0.0001	136	2.99	<0.0001	2.34	<0.0001
	Residual	0.0407	0.00005	864				
S. acuminata	Sex	0.0032	0.0004	8	0.42	0.9057	0.58	0.2688
	Individual	0.1192	0.0009	128	2.13	<0.0001	4.55	0.0260
	Side	0.0064	0.0008	8	1.83	0.076	0.77	0.0196
	Ind * Side	0.0596	0.0004	136	6.20	<0.0001	2.98	<0.0001
	Residual	0.0611	0.00007	864				
S. crassipes	Sex	0.0020	0.0002	8	0.12	0.9982	0.37	0.5707
	Individual	0.3045	0.0020	152	3.26	<0.0001	5.07	<0.0001
	Side	0.0161	0.0020	8	3.27	0.0017	0.32	0.6268
	Ind * Side	0.0984	0.0006	160	9.87	<0.0001	3.70	<0.0001
	Residual	0.0628	0.00006	1008				

Supplementary Table 7. Procrustes ANOVA of the size of the forcipular tarsungulum, without semilandmarks.

Species	Effect	SS	MS	df	F	p
T. nepalensis	Sex	28.83	28.83	1	0.00	0.9900
	Individual	2675137.11	178342.47	15	80.63	<0.0001
	Side	6867.34	6867.34	1	3.10	0.0972
	Ind * Side	35390.29	2211.89	16	20.92	<0.0001
	Residual	10786.47	105.75	102		
S. gracilis	Sex	71325.41	71325.41	1	2.76	0.1141
	Individual	465618.65	25867.70	18	85.47	<0.0001
	Side	189.91	189.91	1	0.63	0.4381
	Ind * Side	5750.71	302.67	19	45.81	<0.0001
	Residual	792.77	6.61	120		
S. linearis	Sex	147306.61	147306.61	1	0.63	0.4406
	Individual	3768930.76	235558.17	16	607.97	<0.0001
	Side	4.52	4.512	1	0.01	0.9153
	Ind * Side	6586.64	387.45	17	13.95	<0.0001
	Residual	2999.66	27.77	108		
S. acuminata	Sex	4132.03	4132.03	1	0.19	0.6673
	Individual	344804.17	21550.26	16	136.38	<0.0001
	Side	807.49	807.49	1	5.11	0.0372
	Ind * Side	2686.37	158.02	17	7.36	<0.0001
	Residual	2319.21	21.47	108		
S. crassipes	Sex	45045.82	45045.82	1	0.36	0.5571
	Individual	2396185.61	126115.03	19	129.48	<0.0001
	Side	4723.41	4723.41	1	4.85	0.0396
	Ind * Side	19479.86	973.99	20	35.4	<0.0001
	Residual	3467.15	27.52	126		

Supplementary Table 8. Procrustes ANOVA of the shape of the forcipular tarsungulum, without semilandmarks.

Species	Effect	SS	MS	df	F	p	Pillai's Trace	Pillai's Trace p
T. nepalensis	Sex	0.0172	0.0086	2	1.30	0.2872	0.14	0.3464
	Individual	0.1980	0.0066	30	5.15	<0.0001	1.64	<0.0001
	Side	0.0014	0.0007	2	0.55	0.5815	0.06	0.6312
	Ind * Side	0.0410	0.0012	32	20.97	<0.0001	1.54	<0.0001
	Residual	0.0125	0.00006	204				
S. gracilis	Sex	0.0059	0.0029	2	0.98	0.3858	0.10	0.4076
	Individual	0.1085	0.0030	36	4.73	<0.0001	1.60	<0.0001
	Side	0.0050	0.0025	2	3.94	0.0278	0.38	0.0141
	Ind * Side	0.0242	0.0006	38	10.33	<0.0001	1.24	<0.0001
	Residual	0.0148	0.0001	240				
S. linearis	Sex	0.0026	0.0013	2	1.18	0.3192	0.09	0.4849
	Individual	0.0356	0.0011	32	2.74	0.0023	1.35	0.0130
	Side	0.0027	0.0013	2	3.27	0.0502	0.24	0.1129
	Ind * Side	0.0138	0.0004	34	3.79	<0.0001	0.85	0.0527
	Residual	0.0232	0.0001	216				
S. acuminata	Sex	0.0024	0.0012	2	0.53	0.5933	0.07	0.5706
	Individual	0.0718	0.0022	32	2.47	0.0054	1.40	0.0052
	Side	0.0003	0.0002	2	0.18	0.8340	0.02	0.8752
	Ind * Side	0.0309	0.0009	34	6.33	<0.0001	0.99	<0.0001
	Residual	0.0310	0.0001	216				
S. crassipes	Sex	0.0012	0.0006	2	0.10	0.9074	0.01	0.9319
	Individual	0.2374	0.0062	38	3.23	0.0002	1.47	0.0006
	Side	0.0173	0.0086	2	4.47	0.0177	0.26	0.0601
	Ind * Side	0.0774	0.0019	40	14.39	<0.0001	1.34	<0.0001
	Residual	0.0339	0.0001	252				

Supplementary Table 9. MANOVA of the shape of the forcipular coxosternite.

Species	Effect	Pillai's Trace	PT p
T. nepalensis	*Symmetric component of shape variation*		
	Sex	0.20	0.8441
	Individual	4.81	<0.0001
	Asymmetric component of shape variation		
	Sex	0.42	0.3787
	Side	0.61	0.0625
	Ind * Side	3.90	<0.0001
S. gracilis	*Symmetric component of shape variation*		
	Sex	0.26	0.6110
	Individual	5.08	<0.0001
	Asymmetric component of shape variation		
	Sex	0.54	0.0786
	Side	0.54	0.0595
	Ind * Side	4.18	<0.0001
S. linearis	*Symmetric component of shape variation*		
	Sex	0.58	0.0833
	Individual	4.57	<0.0001
	Asymmetric component of shape variation		
	Sex	0.24	0.7435
	Side	0.53	0.1100
	Ind * Side	3.35	<0.0001
S. acuminata	*Symmetric component of shape variation*		
	Sex	0.37	4.386
	Individual	4.32	<0.0001
	Asymmetric component of shape variation		
	Sex	0.17	0.8846
	Side	0.37	0.3839
	Ind * Side	3.95	<0.0001
S. crassipes	*Symmetric component of shape variation*		
	Sex	0.15	0.8515
	Individual	4.57	<0.0001
	Asymmetric component of shape variation		
	Sex	0.06	0.9868
	Side	0.57	0.0280
	Ind * Side	4.15	<0.0001